JOURNAL OF MATERIALS SCIENCE 20 (1985) 4139–4146

Damage parameters of lamellar grey cast iron in tension

A. FONTAINE*, G. ZAMBELLI
Ecole Polytechnique Fédérale de Lausanne, 34ch de Bellerive, CH 1007, Lausanne, Switzerland

The tensile rupture behaviour of lamellar grey cast iron depends on the overall damage process of the heterogeneous microstructure. It is therefore of interest to apply the "continuum damage mechanics" concept to this type of material. Two parameters are considered: firstly the damage limit, σ_0, and the damage rate, B. Measurements made on a grey cast iron, cast in three different cross-sections, show that these damage parameters may be used to separate the graphite network effects from those of the matrix which interact in the degradation process of the heterogeneous microstructure of lamellar grey cast iron.

1. Introduction

Numerous recent publications on propagation resistance of macroscopic defects (toughness) in lamellar grey cast iron show two distinct approaches: (1) direct application of standard toughness tests and correlation of the results with microstructural parameters or tensile behaviour [1], and (2) critical study of the validity of those standard toughness tests involving the choice of a crack length most suitable for characterizing the overall damage state specific to this kind of material [2, 3]. This second approach has shown that rupture behaviour in specimens with notches cannot be represented simply by the propagation of a crack. In fact, the total volume under stress is damaged by microcracking of the graphite lamellae and by plastic tearing of the matrix ligaments. This degradation process leads to the formation of a macroscopic defect [2].

From the same basis, some authors have evaluated the rupture behaviour of lamellar grey cast iron in terms of its tensile and compression properties [4, 5]. Using these properties in a finite elements calculation for a simply shaped specimen, these authors predict experimental rupture values by introducing the concept of a calculated "overstressed zone". This concept has already been used [6] in order to model the behaviour of various materials near a sharp notch.

From a critical analysis of these preceding publications, it seems that a characterization of the fracture behaviour of lamellar grey cast iron following the linear fracture mechanic theory or the J integral concept is debatable. This characterization is equally limited when using only the mechanical behaviour laws.

A new approach is proposed in this paper based on "continuum damage mechanics" and using simple assumptions. In the case of uniaxial tension, this concept begins with the real microstructure of a specimen in order to deduce the macroscopical rupture behaviour of the lamellar grey cast iron. The basic essentials of continuum damage mechanics are presented and applied with acceptable simplifications to lamellar grey cast iron so as to determine the damage parameters. The study of the damage process was carried out on three differently cast sections in order to separate effects of the graphite network and the matrix.

2. Continuum damage mechanics

Following the work of Rabotnov and Katchanov, a new internal variable, degree of damage

Present address: Institut de Recherche de la Sidérurgie (IRSID), St-Germain-en-Laye, France.

0022–2461/85 $03.00 + .12

D, was introduced into continuum mechanics. This parameter characterizes the amount of deterioration suffered by a material as shown by its loss of strength. Variation in this parameter shows the transition between the initial state of the material and the formation of macroscopic defects.

Katchanov [7] introduced the idea of "effective stress", $\tilde{\sigma}$, which represents the real stress inside the damaged specimen. The damage parameter, D, was introduced as a variable acting on the stress,

$$\tilde{\sigma} = \frac{\sigma}{1 - D} \quad (1)$$

where σ is the applied stress.

To measure the value of D, the assumption must be made that the deformation of the material remains the same once damaging occurs [8]. Thus, if the initial material can be described by a linear elastic behaviour,

$$\sigma = \varepsilon E_0 \quad (2)$$

where E_0 is Young's modulus, the behaviour of the damaged material can be given by the relationship,

$$\tilde{\sigma} = \varepsilon E_0 \quad (3)$$

If this term for $\tilde{\sigma}$ is substituted into Equation 1,

$$\sigma = \varepsilon \tilde{E} \quad (4)$$

where

$$\tilde{E} = E_0 (1 - D)$$

$\tilde{E}$ is the residual stiffness of the damaged material.

Finally, it is possible to estimate the value of D by partial unloading of the specimen during tensile testing and by the equation:

$$D = 1 - \frac{\tilde{E}}{E_0} \quad (5)$$

Although unidimensional, the above treatment has already been successfully used for several metals as well as for concrete [9].

3. Damage in lamellar grey cast iron

In order to apply the continuum damage mechanics to lamellar grey cast iron, three principal assumptions must be made.

1. No change of existing damage occurs during partial unloadings performed in order to measure the residual stiffness of the material.

2. The macroscopic deformation measured by extensometry is equal to the mean deformation applied to each microscopic volume of the test specimen.

3. The damage is sufficiently homogeneous to permit a unidirectional analysis of the deformation behaviour.

The validity of the first assumption has been supported by recent work which shows that the asymmetry of the hysteresis registered during complete unloading of a lamellar grey cast iron in tension was due to a compression loading of some of the previously cracked graphite lamellae [10]. By means of a rheological model, the same authors have shown that this phenomenon appeared only with large unloading when a fraction of the load was applied (e.g. less than 25%) [11].

The validity of the second assumption was confirmed by tensile tests with small specimens in a scanning electron microscope (SEM). Cracking of graphite lamellae was observed on the entire surface. The damage mechanisms were localized in a definite section only near the maximum load, after a significant reduction of the effective section.

The third assumption requires more detailed examination. The unidimensional description (Equation 5) may be applied to a three-dimensional state even though experimental observations show that the damage in grey cast iron is anisotropic at the macroscopic and microscopic states as long as damaging is isotropic. In order to quantify the degree of anisotropy, the analysis of Chaboche [12] was used which states that the degree of anisotropic damage may be estimated by means of the parameter γ, defined as:

$$\gamma = \left(1 - \frac{\nu}{\tilde{\nu}} \frac{\tilde{E}}{E_0}\right) \Big/ \left[1 - \frac{\tilde{E}}{E_0} \frac{(1 - \nu - 2\nu^2)}{(1 - \nu - 2\nu\tilde{\nu})}\right] \quad (6)$$

where E_0 and ν are Young's modulus and Poisson's ratio for the material before testing, and $\tilde{E}$ and $\tilde{\nu}$ are the residual stiffness and Poisson's ratio of the damaged material, respectively. Furthermore, the (scalar) damage parameter D is defined by:

$$D = 1 - \frac{\tilde{E}}{E_0} \left(\frac{1 - \nu - 2\nu^2}{1 - \nu - 2\nu\tilde{\nu}}\right) \quad (7)$$

In order to check the third assumption, results of

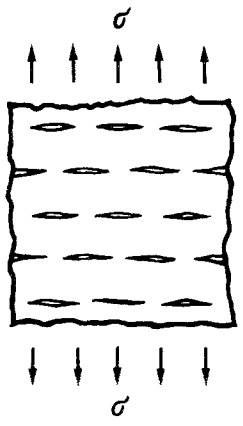

Figure 1 Ideally anisotropic damage induced by microcracks extending plane and normal to the maximum applied tensile stress.

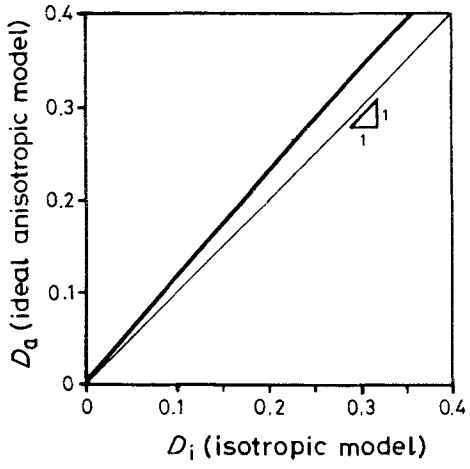

Figure 2 Comparison of the damage parameter D calculated in the case of an ideal anisotropic damage process (D_a) and an ideal isotropic one (D_i). Calculations were made from Gilbert's results [13].

Gilbert [13] concerning the change in stiffness and Poisson ratio measured on lamellar grey cast iron under tensile testing, have been used. These results show that $\tilde{\nu}/\nu = \tilde{E}/E$ and in that case $\gamma \simeq 0$. This is important because Chaboche [12] has shown that $\gamma = 0$ corresponds to ideally anisotropic or "transversally isotropic" damage (Fig. 1). This theoretical deduction is confirmed by microscopic observations which show that only lamellae or portions of lamellae normal to the tensile direction are cracked in the particular case shown schematically in Fig. 1.

The damage parameters D_a and D_i (where D_a is for the anisotropic model, and D_i for the isotropic model) were calculated using Gilbert's results to estimate the error of employing a unidimensional analysis instead of a 3-D one (Fig. 2). At maximum values, D_a and D_i differ by less than 10%. Therefore, for simplification, the unidimensional analysis was employed and the damage parameter, D_i, was chosen (henceforth referred to as D) to quantify damage in lamellar grey cast irons under uniaxial tension.

4. Microstructural examinations

In grey cast iron, uniform microstructures can be obtained in large section castings by the addition of small amounts of alloying elements and appropriate innoculants. The composition of industrial grey cast iron used for various castings is given in Table I. In order to produce various lamellar graphite networks, castings were made in three different section thicknesses: no. 3 (120 mm), no. 4 (40 mm) and no. 5 (20 mm). The microstructure consisted of type A graphite in a pearlite matrix.

As seen in Table I, from the average lengths of the graphite lamellae in the three sections there is a significant difference between the graphite networks. A statistical analysis of lamellae distributions showed that the probability density of their population obeyed a log normal relationship (Fig. 3). The distributions of the lamellae lengths showed a large scatter and are partially superimposed. Therefore, a description of the graphite network solely in terms of an average length is insufficient.

The addition of a small amount of nickel increases the homogeneity of the pearlitic matrix

TABLE I Composition and casting conditions for grey cast-iron

Material	Casting thickness (mm)	Average lamellae length (μm)	Composition (%)				
			C	Si	Ni	Mn	P
3	120	115 ± 5	3.22	1.62	1.13	0.53	0.028
4	40	100 ± 5	3.40	1.66	1.13	0.56	0.030
5	20	60 ± 5	3.28	1.62	1.13	0.55	0.030

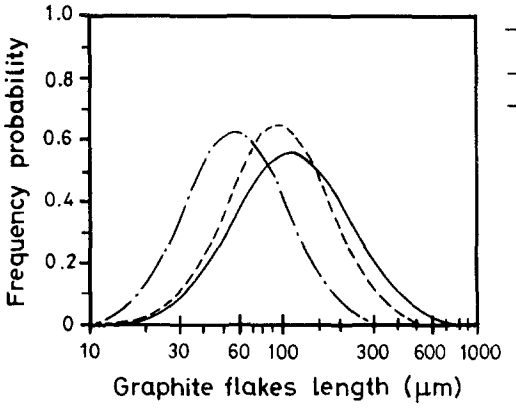

Figure 3 Frequency probability distribution of the graphite flake lengths as measured on a polished surface for three section thicknesses. Note the logarithmic scale for the graphite flake lengths.

independent of the section thickness. Nevertheless, plate 3 was made to contain about 20% ferrite. A progressive ferritizing treatment was carried out on samples from the three plates to identify damage process effects of changes in matrix properties (Fig. 4).

During the ferritizing heat treatment, part of the carbon from the cementite (Fe_3C) was deposited as graphite on the primary graphite lamellae. As the volume fraction of graphite increased, Young's modulus, E_0, decreased with the decrease of the pearlite content (Fig. 5) despite the fact that Young's modulus of the matrix increased slightly.

An estimated increase of 30% in the volume fraction of graphite leads to a reduction of 15 to 20% of the Young's modulus [14]. Fig. 6 shows the agreement between the calculated (straight line) and measured (symbols) decreases in Young's modulus in the case of these alloys. The assumption can be made that the secondary graphite is uniformly deposited on the primary lamellae and since the thickness of these lamellae is less than 5 μm, the length of the lamellae may be considered to be unchanged after ferritizing.

5. Damage laws

Specimens of 6 mm diameter were used for the uniaxial tensile tests; the strain was measured by means of a gauge extensometer over an initial length of 20 mm. The tests were performed at a relatively high imposed strain rate ($\dot{\varepsilon} = 5 \times$

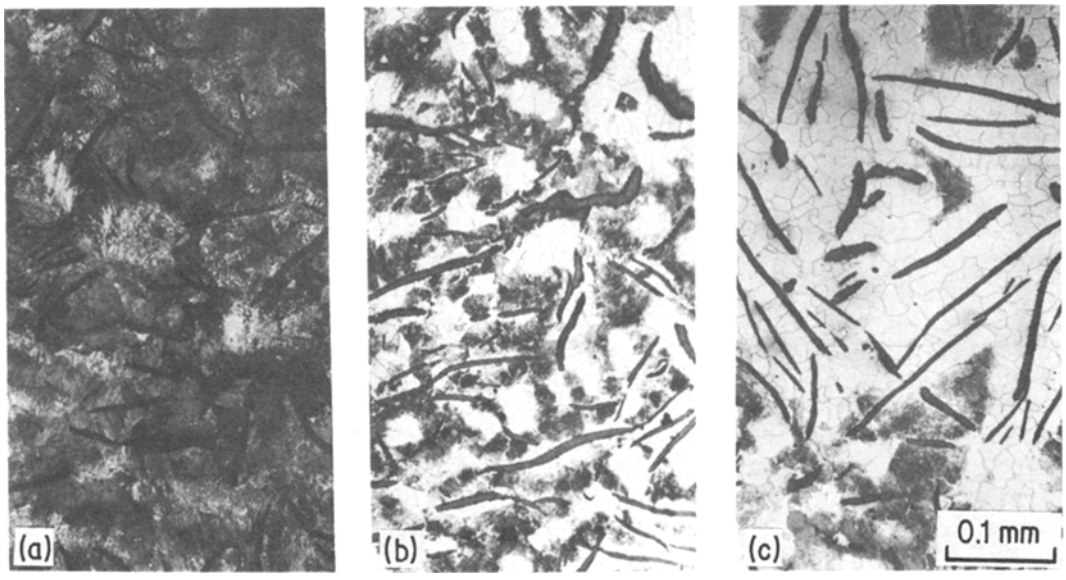

Figure 4 Grey cast iron No. 4 (thickness 40 mm): (a) as-cast, 100% pearlite; after increasing ferritizing heat treatment, (b) 50% pearlite, (c) 20% pearlite. Note that ferrite first appears around the graphite flakes, inducing the deposition of secondary graphite.

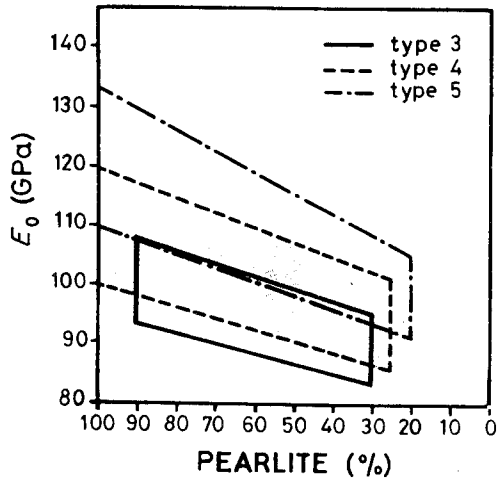

Figure 5 Change in Young's modulus of the flake graphite cast iron studied with the pearlite content of the matrix.

$10^{-4}\,\mathrm{sec}^{-1}$) in order to minimize any possible creep effects. Periodic partial unloadings were made to allow estimations of the residual stiffness of the specimens.

Fig. 7 shows an example of the results obtained from 20% pearlitic matrix grey cast iron (plate 3). The tensile curve and the change in stiffness of the specimen (expressed in % of the Young's modulus E_0 estimated at very low loads) are given in Fig. 7a

With strain rate-controlled experiments, stable fracture progression could be obtained in the majority of specimens. For reasons mentioned in the preceding section, the recordings made after the maximum load was applied were not analysed, since these measurements (or changes in stiffness) relate to the degradation of a limited zone rather than the whole volume within the gauge length.

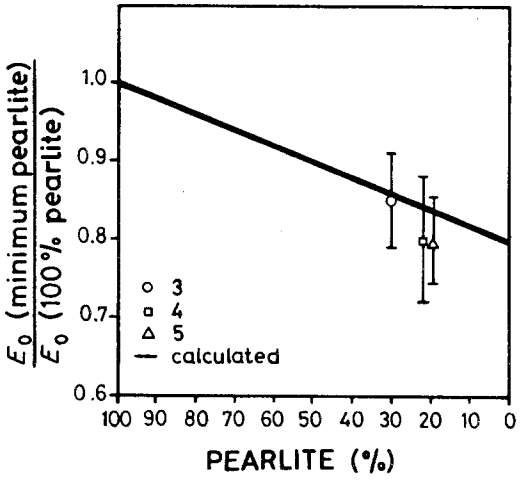

Figure 6 Comparison between the calculated and the measured decrease of the Young's modulus of the alloys. Calculations were based on a linear law of mixing for accounting of the properties of pearlite–ferrite–graphite materials.

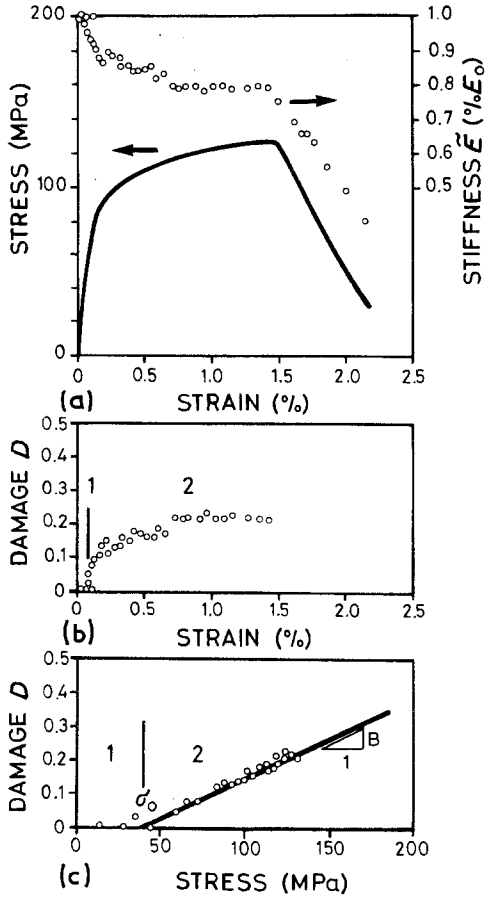

Figure 7 Example of result obtained on a 20% pearlitic matrix–grey cast iron: (a) conventional stress–strain law and change in stiffness (% of Young's modulus); (b) damage parameter D as a function of total strain; and (c) as a function of nominal stress. Note that stages 1 and 2 are the same in (b) and (c) and that in the second case it is possible to find a linear regression between the data for $D \neq 0$.

For each partial unloading, the parameter, D, was calculated from the measured change in stiffness, $\tilde{E}$, by means of Equation 5. The damage D may be expressed in terms of the total strain (Fig. 7b) or of the nominal stress (F/S_0, Fig. 7c), where S_0 is the initial area.

The change in damage, D, as a function of the total strain may be divided into two stages (Fig. 7b): the first stage, difficult to identify, where $D \simeq 0$; the second stage where D increases rapidly and reaches a constant value before the

maximum load is applied. In the first stage it is difficult to define a damage limit, below which the specimen may be loaded without any macroscopic damage. The second stage may be explained by deformation mechanisms of lamellar grey cast iron.

Initially, the rapid increase of parameter D is due to an opening of all or some of the graphite lamellae normal to the tensile direction. Then, strain hardening of the matrix at the extremities of the graphite lamellae prevents further opening and the damage reaches a stationary level. When the matrix can no longer support the increasing strain, the remaining ligaments break after ductile tearing and cracks propagate, thereby rapidly localizing the deformation within a necked region. This is accompanied by a decrease in the applied nominal stress.

The change in D appears differently when expressed as a function of the normal nominal stress (Fig. 7c). The following stages were found: (i) an easily defined first stage where $D \simeq 0$; and (ii) a second stage where D can be approximated by a linear function of stress.

The relationship between D and σ is of interest even though several mechanisms cannot be distinguished in the damage process.

The macroscopic deformation was localized ($> 0.5\%$) and it was not possible to correlate this deformation with the entire volume. Moreover, the variation of D in relation to σ becomes more simple.

Using the method of least squares, the change in D can be approximated. The slope, B, is the rate as a function of stress $\mathrm{d}D/\mathrm{d}\sigma$. By extrapolating this linear regression with $D \neq 0$, a limit σ_0 may be defined below which the damage state remains close to zero. Below this value, the specimen maintains a stiffness close to Young's modulus, which is the usual mechanical property. It should be noted that Gilbert [13] has proposed such a limit of proportionality.

The damage imposed during uniaxial tension on lamellar grey cast iron may therefore be studied by use of the following equations:

$$\begin{aligned} \sigma &\leqslant \sigma_0 \qquad D \neq 0 \\ \sigma &> \sigma_0 \qquad D = B(\sigma - \sigma_0) \end{aligned} \tag{8}$$

The calculated values of σ_0 and B are dependent on the accuracy of the experimental measurements of stiffness made at low stress levels. The scatter of results between different tests from specimens of the same casting may be greater than that due solely to the microstructure. The experimental results are not given as a series of discrete points (calculated average values) but rather as a region showing the maximum calculated variations of the parameters. These regions represent for each casting a minimum of twenty experimental measurements together with the calculation of errors. Although this presentation places a great deal of emphasis on the scatter of the results, it does provide for a better visualization of the general trends of the microstructure–properties relationship and therefore facilitates an analysis of the results.

6. Experimental results

The variation of the damage parameters, σ_0 and B, for the three cast sections of grey cast iron are shown in Fig. 8 plotted against the percentage of pearlite in the matrix. Changes in the size of the

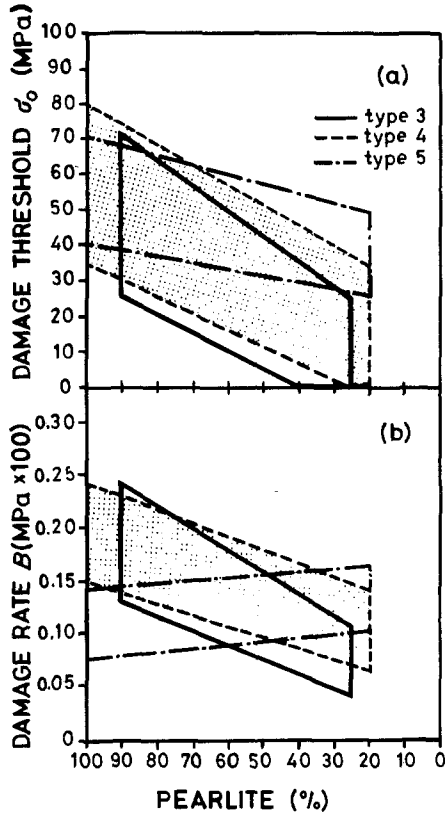

Figure 8 (a) Damage threshold, σ_0, and (b) damage rate, B, as a function of the three graphite networks and the percentage of pearlite of the matrix. The areas include at least 20 experimentally determined σ_0 and B by means of least squares and their errors bars, for each casting thickness.

graphite lamellae do not have the same effect on the values of σ_0 and B in fully pearlitic or fully ferritic matrices. For a purely pearlitic microstructure, changes in the graphite network appear to have little influence on the damage limit ($\sigma_0 \simeq 55$ MPa). The damage limit is practically zero for a 25% pearlite composition with coarsest graphite (plate 3) but reaches 40 MPa with the finest graphite network (plate 5).

Interaction between the graphite network and the matrix microstructures is also evident in the variation of the damage rate B (Fig. 8b).

7. Discussion

In uniaxial tension, the damage suffered by lamellar grey cast iron is related to the cracking mechanisms of a small proportion of the graphite lamellae which are approximately perpendicular to the direction of applied stress.

The volume fraction and the morphology of the graphite influence the initial properties and in particular the initial stiffness, E_0, considered to be Young's modulus. On the other hand, the distribution of the lengths of the lamellae influences the progressive damaging of cast iron under uniaxial tension, in particular the proportion of the longest lamellae perpendicular to the stress field. In fact, linear elastic fracture mechanics shows the stress intensity factor at the lamellae ends, considered as a sharp notch in the matrix, is an increasing function of the length of the lamellae. This effect will therefore be more important for the thicker cast sections which have a significant number of large lamellae (Fig. 3).

The matrix hinders the opening of the graphite lamellae according to its deformation behaviour. Owing to its higher yield stress, the pearlitic matrix is better at detaining the initial opening of the lamellae than a ferritic matrix. This blocking effect is reinforced by the higher level of strain hardening.

The measured damage limit, σ_0, corresponds to a decrease in stiffness due to the opening of a significant number of perpendicular lamellae. When the graphite consists of shorter lamellae, the damage limit, σ_0, must be higher. At a fixed pearlite composition, grey cast iron with fine graphite should have a higher σ_0 than one with coarser graphite lamellae. However, for a pure pearlite matrix, the damage limit remains constant ($\sigma_0 = 55$ MPa) despite the type of graphite network (Fig. 8a). In fact, the effect due to the size of the graphite lamellae is limited by the fracture resistance of the graphite itself.

In ferritic matrices, σ_0 decreases from $\sigma_0 \simeq 55$ MPa to $\sigma_0 \simeq 0$ for a graphitic network having a distribution of large lamellas (no. 3) and 30% pearlite. The microstructure containing the finest graphite (no. 5) keeps a relatively high damage limit, $\sigma_0 \simeq 45$ MPa, with 20% pearlite. The density of large lamellae is the main parameter influencing the damage limit of grey cast iron. The decrease of the elastic strain energy storing capacity between pearlitic and ferritic matrices is not as important if the graphite network remains fine. Heterogeneity in lamellae size distribution is also the more important factor in determining the damage limit, σ_0.

From the definition of the damage rate, B (Fig. 7c), it appears that B is a function of (1) the elastic strain energy stored before the σ_0 is reached, (2) the rate of restitution of energy due to damage, and (3) the rate of increasing the available energy, itself a function of the deformation speed, $\dot{\varepsilon}$. Fig. 8b shows the effect of the interaction graphite network–matrix on the damage rate B for a fixed deformation speed $\dot{\varepsilon} = 5 \times 10^{-4} \text{sec}^{-1}$.

For pearlitic matrices, microstructures containing coarser graphite (no. 3) restore a greater quantity of energy than the finer graphite microstructures (no. 5), although it was observed above that the damage limit σ_0 remained constant irrespective of the population of graphite lamellae. The high values of B measured in microstructures no. 3 and 4 were due to the presence of long open lamellae which produced a greater capacity of energy restitution. Moreover, since the maximum damage, D_{max}, stays practically constant independent of the type of graphite network studied (approximately 0.25), it is possible to estimate the damage rate (slope), B, for the stress interval $\sigma_{max} - \sigma_0$ where damage takes place (Table II). It is obvious that this interval is smaller for microstructures containing coarse graphite (no. 3) which increases the rate of elastic strain energy restitution.

With the partially ferritic matrices (30% pearlite) the intervals of stress ($\sigma_{max} - \sigma_0$) are practically identical for all microstructures examined. This implies that the values of damage rate, B, should be identical but Fig. 8b shows that this is not the case. The estimation of

TABLE II Tensile strengths of pearlitic and ferritic grey cast-iron

Material	Matrix (% pearlite)	Tensile strength, R_m (MPa)
3 (120 mm)	90	170–200
	30	125–155
4 (40 mm)	100	175–205
	30	130–150
5 (20 mm)	100	235–260
	30	165–180

B must be corrected for the difference in strain hardening of pearlitic and ferritic matrices.

8. Conclusion

The application of damage mechanics to the study of the fracture behaviour of grey cast iron provides a quantitative explanation of the progressive damaging in relationship with the heterogeneous microstructure of the material.

The study of the change in damage, D, as a function of the applied stress within a volume element has led to the definition of a damage limit, σ_0, and a damage rate, B, which are dependent on the graphite network–matrix interaction.

The values obtained for these parameters confirm the improved damage strength of a lamellar grey cast iron with fine graphite networks and pearlitic matrices. Considering the tensile strength, R_m, as a limit of fracture resistance (Table II), there is no direct link between the evolution of the damage limit, σ_0, and the variation of R_m. This last measure depends on the ultimate stages of rupture controlled by a complex coalescence of the damaging process in a localized volume. In fact, the fine graphite–pearlitic microstructure had a higher tensile strength than was found for coarser graphite–pearlitic microstructure even though their damage limits were practically identical.

The effect of ferritizing coarse and fine graphite microstructures is not evident when tensile strengths are measured. From continuum damage mechanics analysis, the damage limit σ_0 is practically zero for the coarser graphite network. This observation corresponds to the opening of graphite lamellae at very low levels of stress.

The application of damage mechanics to materials with heterogeneous microstructures, such as grey cast iron, opens up interesting possibilities for a better quantification of the influence of these microstructures on the rupture behaviour.

Acknowledgement

This work was supported by the Swiss National Science Foundation within the framework of the national research programme, "Raw Materials and Materials Problems".

References

1. L. GRÜTER, *Mat. Sci. Eng.* **35** (1978) 157.
2. L. HAENNY and G. ZAMBELLI, *Amer. Foundrymen's Soc. Trans.* **82-36** (1982) 275.
3. *Idem, Eng. Fract. Mech.* **21** (1985) 529.
4. T. NOGUCHI and K. NAGAOKA, *Amer. Foundrymen's Soc. Trans.* **82-64** (1982) 323.
5. *Idem, Bull. Faculty Eng. Hokkaido Univ.* **112** (1983) 1.
6. V. WEISS, "Notch analysis of fracture in Fracture", edited by Liebowitz (1971), (Academic Press, New York, 1971) pp. 227–64.
7. L. M. KACHANOV, *Izv. Akad. Nauk. S.S.R. Otd. Tekh. Nauk.* **8** (1958) 26.
8. J. LEMAÎTRE and J. C. CHABOCHE, *J. Méc. Appl.* **2** (1978) 317.
9. J. LEMAÎTRE and J. MAZARS, *Ann. Inst. Tech. Bâtiment et Trav. Pub.* **401** (1982) 114.
10. L. HAENNY and G. ZAMBELLI, *Eng. Fract. Mech.* **18** (1982) 377.
11. *Idem, ibid.* **19** (1983) 113.
12. J. L. CHABOCHE, *Nucl. Eng. Des.* **64** (1981) 233.
13. G. N. J. GILBERT, *Brit. Foundryman* **61** (July) (1968) 264.
14. G. R. SPEICH, A. J. SCHWOEBLE and B. M. KAPADIA, *J. Appl. Mech.* **47** (1980) 821.

Received 10 December 1984
and accepted 15 January 1985